Effects of fullerene on lipid bilayers displaying different liquid ordering: a coarse-grained molecular dynamics study

Judit Sastre,[§] *Ilaria Mannelli,*[#] *and Ramon Reigada*[*,§,¶]

§Departament de Ciència dels Materials i Química Física, Universitat de Barcelona, c/ Marti i Franqués 1, Pta 4, 08028 Barcelona, Spain

#ICFO-Institut de Ciències Fotòniques, The Barcelona Institute of Science and Technology, 08860 Castelldefels (Barcelona), Spain

¶Institut de Química Teòrica i Computacional (IQTCUB), Universitat de Barcelona, c/ Marti i Franqués 1, Pta 4, 08028 Barcelona, Spain.

ABSTRACT

Background:

The toxic effects and environmental impact of nanomaterials, and in particular of Fullerene particles, are matters of serious concern. It has been reported that fullerene molecules enter the

cell membrane and occupy its hydrophobic region. Understanding the effects of Carbon-based nanoparticles on biological membranes is therefore critical to determine their exposure risks.

Methods:

We report on a systematic coarse-grained molecular dynamics study of the interaction of fullerene molecules with simple model membranes. We have analyzed bilayers consisting of lipid species with different degrees of unsaturation and cholesterol fractions. Addition of fullerene to phase-segregated ternary membranes is also investigated in the context of the lipid raft model for the organization of the cell membrane.

Results:

Fullerene addition to lipid membranes modifies their structural properties like thickness, area and internal ordering, as well as dynamical aspects such as molecular diffusion and cholesterol flip-flop. Interestingly, we show that phase-segregating ternary membranes accumulate fullerene molecules preferentially in the liquid-disordered domains promoting phase-segregation and domain alignment across the membrane.

Conclusions:

Lipid membrane internal ordering determines the behavior and distribution of fullerene particles, and this, in turn, determines the influence of fullerene on the membrane. Lipid membranes are good solvents of fullerene molecules, and in particular those with low internal ordering.

General Significance:

Preference of fullerene to be dissolved in the more disordered hydrophobic regions of a lipid bilayer and the consequent alteration of its phase behavior may have important consequences on the activity of biological cell membranes and on the bioconcentration of fullerene in living organisms.

Keywords

Fullerene; Environmental impact; Lipid membrane; Cholesterol; Lipid raft; Coarse-grained molecular dynamics

1.INTRODUCTION

Carbon nanomaterials are of exceptional importance in nanoscience given their unique electrical, thermal, chemical and mechanical properties [1]. Their range of applications is very wide [1]: composite materials, energy storage and conversion, sensors, drug delivery, field emission devices and nanoscale electronic components. Although the production of nanomaterials is rapidly growing [2] their toxicology and environmental impact are still matters of serious concern [3]. Nanomaterials could possibly enter human cell [4] and, for instance, harmful effects of inhaled nanoparticles on lungs, brain and olfactory bulb have been reported [5-7]. A better understanding of their interaction with biological systems is then required to minimize their adverse effects on living beings.

Since the discovery of fullerene (C_{60}) in 1985, it has become one of the most widespread carbon-based nanomaterials and it has attracted attention in many research fields due to their exclusive properties. Applications of C_{60} and its derivatives range from material science [8] to nanomedicine, in this latter context acting such as X-ray contrast agents [9], antioxidant drugs for neurodegenerative diseases [10], inhibitors of the allergic response [11] and targets for bone tissue [12]. Despite the large variety of uses of fullerene and its increasing worldwide production [13,14] little is known about possible biological negative effects. In fact, strong evidences that fullerenes are cytotoxic have been reported [15-17], and it has been demonstrated that fullerene aggregates can penetrate cells and cross the blood brain barrier [3,6]. It is necessary then to develop empirical and modeling tools to assess the effects of this compound when released to the environment. Since the cell membrane is the first obstacle to overcome when interacting with living beings, a better understanding of the mechanism of lipid membrane penetration and membrane alterations due to fullerene interaction is needed. Simple and reproducible systems, such as model lipid membranes, are appropriate to elucidate the physical principles governing these complex interactions. A few experimental studies have been performed on the distribution of fullerene between aqueous solutions and simple solid supported lipid membranes [18,19]. Global descriptors such as the water/lipid partition coefficient clearly evidence the ability of fullerene to be preferentially placed in the lipid phase [18,19], thus confirming its potential bioaccumulation in biological cell membranes. The use of small lipid vesicles as biocompatible platforms for the dispersion of fullerene particles has been also attempted [20,21]. By encapsulating aqueous solutions containing fullerene clusters within vesicles, fullerenes may be transferred to the hydrophobic region of the vesicle bilayer [22] and dispersed as molecular

entities or small nano-aggregates [20]. These lipid/fullerene assemblies have received considerable attention due to their potential biochemical applications [21].

The consequences of fullerene accumulation on cell membranes or its interaction with lipid bilayers, which are often used as model biological membranes, require a deep understanding of the produced effects at the molecular detail. In which parts of the lipid bilayer matrix are the fullerene molecules partitioned once inside the membrane? What are the resulting local and global effects on the lipid bilayer structure as well as on its molecular dynamical properties? How these effects depend on the lipid composition and organization of the membrane lipid matrix? These and other issues have to be analyzed at the molecular detail in order to understand the consequences of fullerene accumulation on the functionality of cell membranes. Molecular dynamics (MD) simulations provide an excellent approach to unveil the ultimate molecular mechanisms regulating the behavior of interacting systems and they have been successfully used to obtain direct insights into many lipid membrane processes. MD simulations using a full atomistic description of the interacting molecules have been already used to study the effects of fullerene molecules on simple lipid bilayers [23,24]. Atomistic MD simulations, however, are limited to short time (a few hundred of ns) and length scales (10-20 nm), whereas coarse-grained (CG) MD covers much longer scales still preserving the main molecular characteristics of the simulated moieties. Recently, a CG model for fullerene has been developed and used for single-lipid bilayer simulations [25-27], unveiling interesting details of the fullerene translocation process through the bilayer and its consequences on some basic membrane properties such as thickness, lipid order, diffusivity and elastic and compressibility moduli [25]. Moreover, CG simulations also show that fullerene clusters can be absorbed from an aqueous solution and

disaggregate once inside the bilayer [25,27]. A detailed analysis provides the molecular clues to explain why lipid bilayers are better solvents for fullerene molecules than similarly apolar alkane moieties [27].

All previous computational studies focused on single-lipid bilayers as model membranes. However, cell membranes of different organisms display different lipid compositions, and even within a single organism, cell lipid composition can vary [28]. Lipid composition determines many membrane properties such as thickness, internal ordering, lipid diffusivity, etc. To take into account this diversity, in this Paper we analyze the effects of fullerene in lipid membranes formed by phospholipid moieties with different degrees of saturation, and containing different fractions of cholesterol -an important component of eukaryotic cell membranes-. Fullerene translocation through the membrane and its partitioning inside the bilayer are analyzed depending on the bilayer characteristics while modification of structural and dynamical membrane properties due to the presence of fullerene molecules are as well studied. Lipid cell membrane composition is also particularly relevant in relation to one of the emergent issues in biophysics: the raft concept for cell membranes [29]. The raft hypothesis is based on the idea that lipids in plasma membranes are distributed inhomogeneously, forming small liquid-ordered (*lo*) domains rich in cholesterol and saturated lipids that are embedded in a liquid-disordered (*ld*) medium preferentially containing unsaturated lipids. Although some aspects of the raft phenomenology remain currently controversial [30], it is well accepted that such structures are implicated in many biological processes [31]. Therefore, fullerene effects on biological cell membranes should consider lipid heterogeneity and *lo*/*ld* coexistence. Consequently, we have

also investigated the behavior of fullerene molecules on phase-segregating membranes consisting of a saturated lipid, an unsaturated lipid and cholesterol.

2.METHODS

2.1 Coarse-grained description and simulated membranes.

The coarse-grained model proposed by the Martini force field is used here to describe the simulated molecules. This model is based on a 4-to-1 mapping where on average four heavy atoms are represented by a single interactive bead, except for ring-like molecules that are mapped with higher resolution (for instance, cholesterol is described by a 3-to-1 resolution) [32]. The Martini model has been successfully applied to study a large variety of lipid membrane phenomena [33-35]. The numerical simulations are carried out for membranes consisting of three phosphatidylcholines (PC) displaying different levels of unsaturation in their acyl chains: DUPC (with two double-unsaturated 16:2 tails), POPC (with an unsaturated oleoyl 18:1 tail and a saturated palmitoyl 16:0 tail) and DPPC (with two saturated palmitoyl 16:0 tails). Each PC is described by a positively charged choline group, a negatively charged phosphate, two neutral glycerols, and two tails with four (for 16 carbon length tails) or five (for the oleoyl tails) apolar particle beads (see Fig. 1). Cholesterol (Chol) is also added to some of the simulated membranes. Chol molecules are described by eight particles: a polar bead for the hydroxyl group, five representing the ring sterol system and two for the short alkyl tail (Fig. 1) [32]. Fullerene molecules are described following the coarse-graining Martini procedure and consisted of 16 apolar beads (F16, Fig. 1). The CG fullerene model was initially developed and tested in single-lipid (DOPC or DPPC) bilayer simulations [25], and later refined by reproducing, at the same

time, the experimental free energies of transfer between different solvents, the fullerene-fullerene interaction energy from detailed atomistic simulations and the experimental sublimation enthalpy [26].

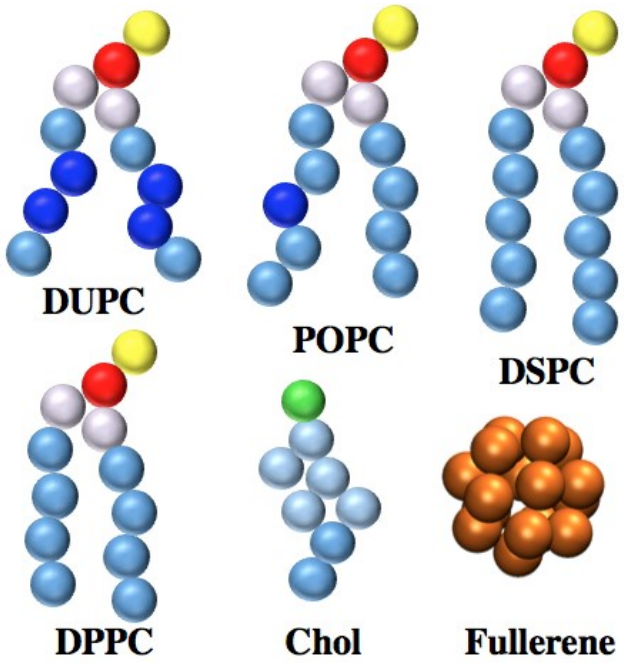

Figure 1. Schematic representation of the simulated molecules according to their CG Martini description. Blue beads correspond to apolar particles forming the PC tails (dark: unsaturated segments, normal: saturated segments) and Chol structure (light: ring structure, normal: saturated ending tail). Yellow, red, white and green beads stand for choline, phosphate, glycerol and hydroxyl groups, respectively. Fullerene is formed by 16 apolar beads (in orange).

The simulated single-lipid membranes are composed of 800 PC molecules, equally distributed in the two leaflets. Membranes with two different fractions of Chol are also simulated: 30 mol% of Chol (576 PCs + 248 Chols) and 50 mol% of Chol (576 PCs + 576 Chols). In all cases, PC and Chol molecules are initially randomly mixed and equally distributed in the two leaflets of the bilayer. To ensure correct hydration, 16000 water Martini particles are used for each membrane

system. Each one of the 9 membrane systems is simulated in the absence of fullerene, and in the presence of 1, 10, 20 and 50 fullerene molecules. The fullerene molecules are initially placed in random positions of the aqueous bulk phase. Each simulated system is generically referred as PC/mol%Chol/num_F16; for instance, the POPC/30%Chol/10F16 system corresponds to a POPC bilayer containing a 30 mol% of Chol and 10 fullerene particles.

2.2 Simulation protocols.

The simulations are performed using the GROMACS v.4.5.5 software package [36]. The simulations are carried out in the NpT ensemble through a weak coupling algorithm at T=310 K and an anisotropic p=1 atm. Electrostatic interactions are handled using a shifted Coulombic potential energy form and charges are screened with a relative dielectric constant ε_r=15. Non-bonded interactions are cut off at 1.2 nm. Periodic boundary conditions are used in all three directions, and the time step is set to 20 fs. Due to the "smoothing" inherent to the coarse-grained potentials, the effective time scale is larger than the actual simulation time. Here we use the standard conversion factor of 4 [32], which is the speed-up factor needed to obtain the correct diffusional dynamics of CG water particles compared with real water molecules. All membrane systems are first equilibrated for 500 ns, and then simulated for a period of 4.8 μs.

2.3 Potential Mean Force simulations.

The free energy profiles (potential of mean force, PMF) for a fullerene molecule traversing the simulated lipid bilayers are calculated using the umbrella sampling method [37]. Smaller membranes are used for this purpose: 200 PCs for the single-lipid bilayers, 144 PCs + 62 Chols for the 30 mol% Chol membranes, and 144 PCs + 144 Chols for the 50 mol% Chol bilayers. In all cases, the membranes are sufficiently hydrated with 4000 water particles. Once the systems

were equilibrated the PMF(z) is calculated for a length of 8 nm traversing the membrane in a series of 100 independent simulation windows with the center of mass of fullerene fixed by a harmonic constraint around z positions in 0.08 nm steps. Each umbrella simulation window is performed for 800 ns (200 ns of equilibration). The analysis of the umbrella simulations is performed using the weighted histogram analysis method (WHAM) [38].

2.4 Raft membrane simulations.

Two ternary membrane systems are initially built as a random mixture of the 828 DUPC molecules (42.6 mol%), 540 saturated PC molecules (27.8 mol%) and 576 Chol molecules (29.6 mol%), equally distributed in the two leaflets. Two saturated PC lipids with different tail lengths have been considered: DPPC (with two saturated 16:0 tails) or DSPC (with two saturated stearoyl 18:0 tails, see Fig. 1). The two membranes are conveniently hydrated with 22000 water particles, and they are equilibrated for 18 μs using the temperature and pressure conditions described in Section 2.2. In order to analyze the effects of fullerene, 100 and 200 F16 molecules are randomly added to the water phase of each equilibrated ternary membrane system, and the simulations are then conducted for an extra time period of 4.8 μs.

Visual inspection of the equilibration process before fullerene addition reveals a clear phase segregation process for the two simulated ternary membranes: the saturated lipid forms a packed lipid phase (*lo*) together with Chol molecules, segregated from a disordered phase (*ld*) rich in the unsaturated lipid (DUPC) [34]. The difference between the two simulated raft systems is related to the correlation between membrane leaflets. As it was already shown in previous CG MD simulations [34, 39], the membrane containing the longest-tail lipid (DSPC) shows a clear phase

antiregistration behavior (*lo* and *ld* are not aligned in the two leaflets), whereas the membrane containing DPPC displays an alignment of the segregating domains (phase registration).

We want to analyze the effect of fullerene on both aspects of the membrane phase behavior: the stability of the lateral (in-plane) segregation process and the correlation of *lo* and *ld* domains at both leaflets of the membrane. With this purpose, Voronoi tessellation of each membrane leaflet has been performed according to the plane projections of phosphate beads of PC molecules and hydroxyl groups of Chol molecules. Because each Voronoi polygon is associated with an individual molecule, lateral (in the same leaflet) and transversal (in opposite leaflets) neighbors can be readily assigned to each membrane molecule. The *lo*/*ld* segregation process is quantitatively tracked by means of a segregation parameter Φ that corresponds to the fraction of lateral contacts between lipid molecules corresponding to the same phase [34]. DUPC molecules are considered to form the *ld* phase, whereas the saturated PC species correspond to the *lo* phase. Cholesterol molecules are considered to be part of the *lo* phase except in the cases where they have more DUPC neighbors than saturated and other Chol molecules. Strong segregation is characterized by values of Φ closer to 1. Similarly, an interleaflet coupling parameter Λ can be computed in order to quantify the transversal alignment of segregating domains [34]. Each lipid molecule has a unique transmembrane neighbor, so the local interleaflet coupling parameter Λ corresponds to the fraction of transversal neighbors of the same lipid phase. Values of $\Lambda \to 1$ correspond to registration (phase alignment) of lipid domains, whereas small values of Λ stand for antiregistration of segregating phases.

3.RESULTS and DISCUSSION

3.1 Fullerene translocation.

As general behavior, fullerene molecules translocate to the membrane by traversing the interfacial headgroup polar region and become placed diffusing in its hydrophobic sector. After internalization, fullerene molecules were never observed to return to the aqueous phase during the simulation time in any of the simulated membrane systems. The translocation process depends on the compactness of the bilayer. For example, 10 fullerene molecules are transferred to the DUPC membrane (the most fluid and least condensed) in single-particle fast (fractions of nanosecond) adsorption events after 214 ns (Fig. 2). Fullerenes require more time to penetrate more packed membranes: adsorption of the 10 fullerene particles took place after 912 ns in the DPPC bilayer (Fig. 2). In this case, a cluster of 6 fullerenes was formed in the aqueous phase and traversed the headgroup interface in about 10 ns. In Fig. 3, the translocation dynamics for the membranes interacting with 10 fullerenes is analyzed so the general characteristics of this process can be noticed. First, by using PC lipids with a higher melting point (DPPC > POPC > DUPC), the membranes become more packed, and the translocation process takes longer (upper panel in Fig. 3). Second, addition of cholesterol increases the membrane compactness, thus the adsorption of all fullerenes is completed at longer times (Fig. 3). Such cholesterol effect is more pronounced for membranes consisting in saturated (DPPC) and single-unsaturated (POPC) lipids than for highly unsaturated ones (DUPC), which typically do not display a strong cholesterol condensation effect. For less condensed bilayers fullerene translocation generally occurs in fast single-adsorption events whereas for packed ones fullerenes are able to form clusters of a few molecules in the aqueous phase before being transferred to the bilayer. As expected, larger

clusters in packed bilayers traverse the headgroup membrane region slower than smaller ones in less condensed membranes.

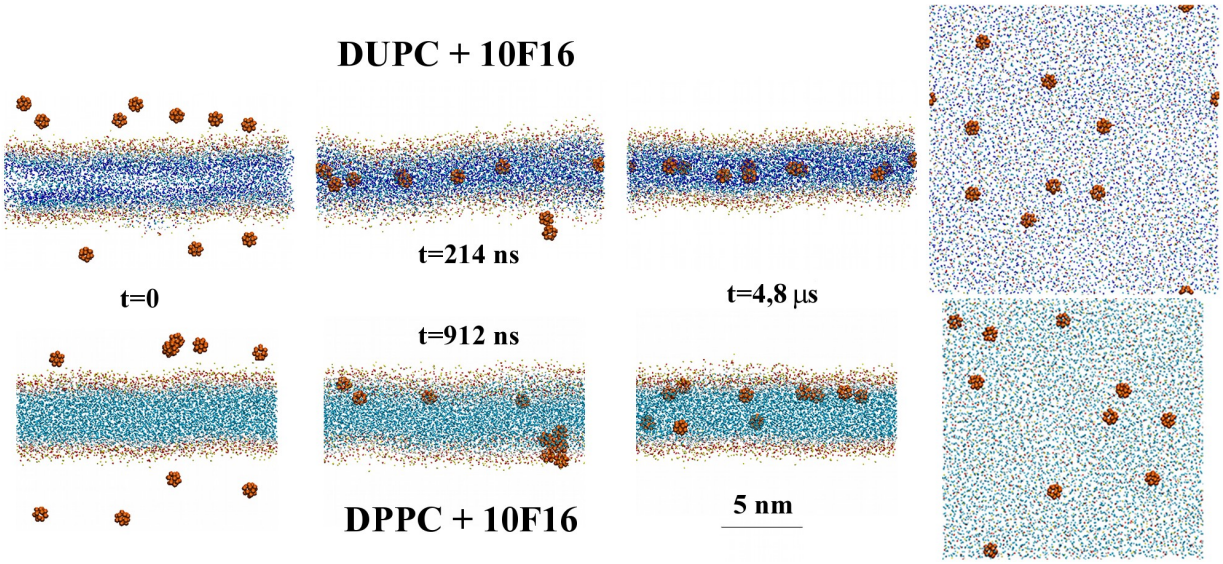

Figure 2. Temporal sequence of the lateral view for a DUPC (up) and DPPC (bottom) membranes with 10 fullerene molecules initially placed in the aqueous phase (left panels). The panels in the second column correspond to the times where the last fullerene molecules entered the membrane. The top views of the final system configurations (panels in the third column) are also provided (right panels). The color code is the same as in Fig. 1. Water molecules are not shown for clarity.

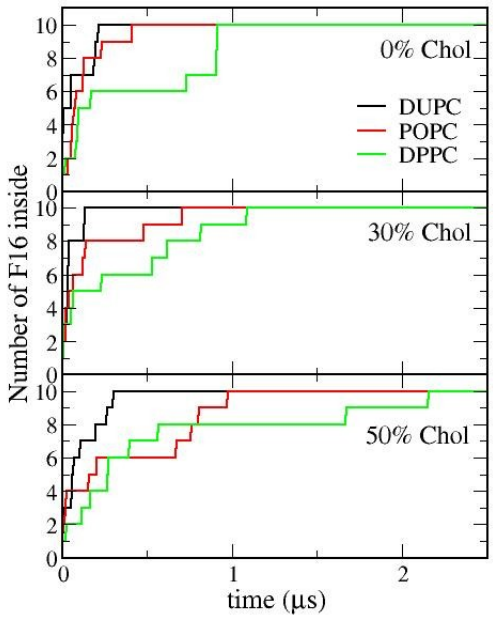

Figure 3. Temporal evolution of the number of fullerene molecules entering the simulated membranes for the cases where 10 fullerenes are added to the aqueous phase.

Once inside a single-lipid bilayer, fullerene molecules are dispersed and adopt a random distribution in the membrane plane, even if they entered as a cluster. Larger clusters require more time to disaggregate inside the bilayer, and this time is also dependent on the membrane compactness. For instance, the six-fullerene cluster observed in Fig. 2 for a DPPC membrane lasts for about 300 ns before loosing completely its integrity. Once disaggregated, however, no further aggregation is observed. In Fig. 4, the nearest-neighbor distance distributions between fullerene molecules inside the bilayer for the single-lipid bilayer simulations (red curves) are plotted, which compares quite well with the random distribution (black curve).

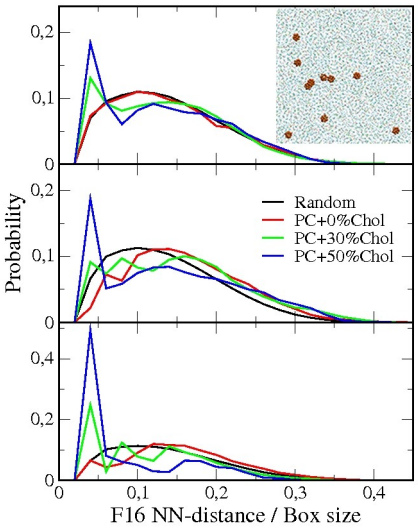

Figure 4. Probability distribution for the fullerene-fullerene nearest-neighbor distances (F16 NN-distance) respect to system linear size. DUPC, POPC and DPPC membranes are presented from top to bottom. The cases with 10 fullerenes are analyzed and the probability distributions were computed averaging the NN-distance once all 10 fullerene particles entered the membrane. In the inset a top view of the DUPC/50%Chol/10F16 membrane is shown.

Remarkably, addition of cholesterol increases the propensity of fullerene to aggregate. Fullerene encounters inside the bilayer are favored by the presence of Chol as noticed from the peak at short distances in the nearest-neighbor distance distributions for bilayers containing cholesterol (green and blue curves in Fig. 4). Cholesterol promotes the formation of small (2-3 fullerenes) clusters that diffuse together but rapidly disaggregate after a few nanoseconds (inset of Fig. 4). Additionally, the presence of cholesterol may also retard or even halt cluster disaggregation once they enter into the membrane, especially for DPPC and POPC bilayers. For instance, in Fig. 5a the DPPC/50%Chol/10F16 system shows a five-fullerene cluster that enters

into the membrane after 620 ns and continues diffusing as a cluster for the remaining simulation period (more than 4 μs). Our simulations, therefore, reveal that Chol reduces the ability of lipid membranes to be good solvents for fullerenes [27] and promotes their aggregation. This effect can be understood in terms of the modification of fullerene/lipid interactions: whereas a PC lipid molecule is able to wrap fullerene individual molecules with their flexible (and hydrophobic) acyl tails, cholesterol is rather a rigid molecule, so that its interaction with fullerene particles is energetically penalized. Consequently, when cholesterol molecules are present in the lipid membrane mixture, fullerene aggregation results in a reduction of non-favorable fullerene/cholesterol contacts, thus explaining the reported observations. A detailed analysis of our simulations evidences a significant bias to avoid fullerene/cholesterol contacts. For instance, we have computed the number of lipid (PC or Chol) molecules that are proximal to fullerene molecules by considering all molecules whose center of mass is closer than 0.8 nm to a fullerene particle. In Table 1 we report the number of proximal PC and Chol particles for each simulated membrane when adding 10 and 20 fullerene molecules. Clearly, for cholesterol-containing bilayers the fraction of proximal Chol molecules is smaller than the global sterol percentage in the bilayer (see Table 1). Furthermore, the number of close contacts (distance<0.5 nm) among the hydrophobic beads of lipid molecules (PC or Chol) and fullerene particles has been computed and reported in Table 1. Again, the relative amounts of fullerene/Chol contacts are smaller than both mass and molar Chol fractions in the membrane. Notice also that this effect is more pronounced for DPPC and POPC since cholesterol interactions with saturated (DPPC) and single-unsaturated (POPC) lipids are particularly favorable: by favoring lipid/lipid (solvent/solvent) interactions, fullerene/fullerene (solute/solute) contacts are prompted.

Table 1. Proximal lipid molecules[a] and contacts with hydrophobic lipid beads[b] per fullerene for different simulated membrane systems and fullerene contents.

PC	%mol Chol	10 F16						20 F16					
		Proximal		%PC	Contacts		%PC	Proximal		%PC	Contacts		%PC
		PC	Chol		PC	Chol		PC	Chol		PC	Chol	
DUPC	0%	5.0	-	100%	13.0	-	100%	5.0	-	100%	13.0	-	100%
	30%	4.8	1.0	82.9%	12.1	2.36	83.7%	4.8	1.0	83.1%	12.0	2.48	82.8%
	50%	4.4	2.5	63,7%	10.4	6.53	61.3%	4.1	2.6	61.9%	10.2	6.30	61.8%
POPC	0%	5.7	-	100%	10.3	-	100%	5.6	-	100%	10.3	-	100%
	30%	5.3	1.5	77,6%	9.85	1.19	89.2%	5.0	1.6	76.5%	9.88	1.38	87.7%
	50%	4.5	3.5	56,7%	9.31	4.35	68.2%	-[c]	-	-	-	-	-
DPPC	0%	6.0	-	100%	9.94	-	100%	5.9	-	100%	9.98	-	100%
	30%	5.8	1.7	76,9%	9.48	1.37	87.4%	4.9	1.4	77.9%	8.88	1.01	89.8%

	50%	4.0	2.8	58.8%	8.26	3.07	72.9%	3.1	2.4	55.5%	6.56	3.15	67.6%

[a]Number of proximal lipid molecules (PC or Chol) per fullerene. A lipid molecule is proximal if its center of mass is closer than 0.8 nm to a fullerene molecule.

[b]Number of close contacts (<0.5 nm) per fullerene between fullerene and lipid (PC or Chol) hydrophobic beads.

[c]In the case POPC50%Chol/20F16, fifteen fullerenes form a cluster in the water phase and do not enter into the membrane during the simulation time.

Finally, for the bilayer systems containing 20 and 50 fullerenes, the formation of fullerene clusters in the aqueous phase is almost assured. Although most clusters enter into the membrane, in some cases, clusters become so large that they can not be transferred to the membrane (at least during the simulated period) and remain diffusing in the aqueous phase. The POPC/50%Chol/20F16 and DPPC/50%Chol/50F16 cases are two examples of this situation and are plotted in Figs. 5b and 5c, respectively. It is important to notice at this point that although fullerene displays a clear tendency to enter and remain inside the lipid bilayer, high densities of this compound may prevent its adsorption due to the formation of large clusters at the aqueous phase before contacting the membrane.

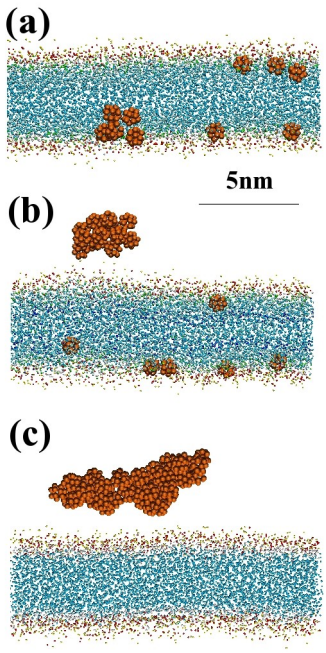

Figure 5. Some cases displaying the persistence of fullerene clusters at the end of the simulated periods: (a) DPPC/50%Chol/10F16, (b) POPC/50%Chol/20F16, (c) DPPC/50F16.

3.2 Fullerene distribution inside the membrane.

Due to its hydrophobic character, fullerene is partitioned into the interior of the membrane, which is occupied by the apolar lipid tails. The precise location inside the bilayer, however, strongly depends on its lipid composition; first, on the PC forming the membrane, and second, on its cholesterol fraction. Single-lipid membranes formed by POPC (monounsaturated) and DPPC (saturated) host fullerene molecules at 1.2 nm and 1.1 nm distance from the center of the bilayer, respectively (Fig. 6a). This location corresponds to the region immediately deeper than the glycerol particles, and for POPC, to the segment between glycerol and double bond bead sectors (Fig. 6a). Similar results were found in atomistic [23,24] and other coarse-grained [25,26] MD simulations. Highly unsaturated DUPC, however, exhibit a strong preference to burry fullerene at the center of the bilayer (Fig. 6a).

Free energy profiles for a fullerene molecule as a function of its distance to the bilayer center of mass display an excellent agreement with fullerene density profiles, see Fig. 6b. In POPC membranes, an energy minimum is found at 1.2 nm implying a stabilization of 82.2 $kJmol^{-1}$ with respect to the water phase (where the PMF is taken as zero) and 2.6 $kJmol^{-1}$ in relation to the maximum in the bilayer center. A similar profile is found for DPPC membranes where the minimum is displaced to 1.1 nm and the energy gains respect to water and the bilayer center are 79.3 and 10.4 $kJmol^{-1}$, respectively. In both cases, a small barrier (3-4 $kJmol^{-1}$) to fullerene penetration is found in the water/PC headgroup interface. DUPC membrane does not display such penetration barrier, and exhibit a single minimum at the bilayer center, according to its preference to dissolve fullerenes in the bilayer midplane region (Fig. 6b). The energy stabilization is 92.2 $kJmol^{-1}$, the largest of the three simulated PCs.

The free energy profiles can be understood as a balance between two opposing effects: the cost of vacating the space to be occupied by the fullerene molecule, and the dispersion interactions resulting from inserting the fullerene into the vacancy [23,40]. The former is reduced at the center of the bilayer where the accessible free volume is larger, whereas favorable dispersion interactions are maximized at the densest regions of the membrane that are usually located immediately below the glycerol backbone. For DPPC and POPC bilayers, the higher number of dispersion interactions promotes the accumulation of fullerenes far from the bilayer center. DUPC is highly unsaturated and it is formed by four unsaturated tail beads that occupy most of the hydrophobic membrane region. Since interactions between fullerene and double bond particles are less favorable (for instance in POPC membranes, fullerenes also avoid contacts with the double bond region), fullerene is driven towards the center of the membrane. Notice in the

upper panel of Fig. 6a, how F16 molecules are placed in the most inner regions where the presence of the deepest double bond beads is reduced.

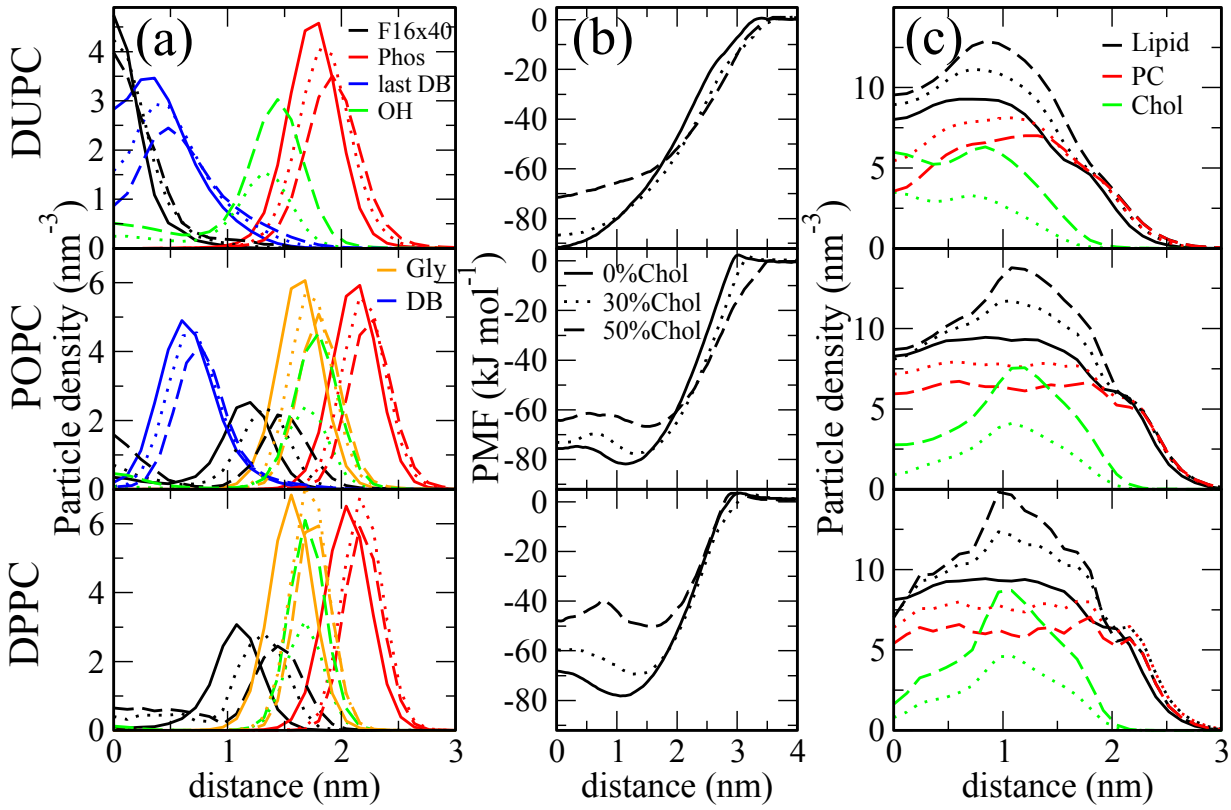

Figure 6. (a) Particle density profiles respect to the bilayer center for the nine simulated membrane systems containing fullerene. Fullerene (F16, black), phosphate (Phos, red), glycerol (Gly, orange) and Chol hydroxyl (OH, green) particle beads are represented. For DUPC the deepest double bond bead (last DB, blue) and for POPC the double bond bead (DB, blue) are also plotted. For clarity, fullerene profiles are multiplied by 40. (b) Potential of Mean Force (PMF) profiles are plotted for a single fullerene molecule as a function of the distance respect to the bilayer center. (c) Particle density profiles for PC (red) and Chol (green) molecules. The total

lipid profiles (black) are also plotted. In all panels, curves in solid, dotted and dashed lines correspond to 0, 30 and 50% Chol molar fractions, respectively. The density profiles shown here correspond to the cases with 10 fullerenes. Simulations with different number of fullerene molecules display similar results.

Addition of cholesterol produces significant effects on the free energy profiles that can be ascribed to the non-favorable interactions with fullerene particles commented above. The first effect is common to all PC membranes and consists in a reduction of the energy gain obtaining by dissolving fullerene inside the membranes. In DUPC bilayers, for instance, the energy minimum is reduced in 5.2 and 21.0 $kJmol^{-1}$ for 30% and 50% Chol molar fraction, respectively (Fig. 6b). Since Chol density profile in a DUPC membrane is rather homogeneous (Fig. 6c), no other effects are found in these systems and the fullerene density profiles are not qualitatively modified. In POPC and DPPC, however, Chol exhibits its highest density around 1 nm of distance to the bilayer center (see Fig. 6c), producing a deviation of the PMF energy minimum towards the lipid headgroup region and also the emergence of an energy minimum at the bilayer center (Fig. 6b). The reduction of favorable dispersion interactions due to the presence of cholesterol pushes some fullerene molecules to the bilayer center where the excluded volume is large and cholesterol is not so abundant (see Fig. 6a).

3.3 Bilayer alterations due to fullerene

Structural bilayer properties have been analyzed for the 10F16 and 20F16 cases. The alterations caused upon fullerene insertion are rather small. For instance, the projected membrane area is increased by a maximum increment of 3.2% once 20 fullerenes are transferred to the membrane and 1.5% after insertion of 10 fullerenes (such maximal increments are observed for DPPC/Chol membranes). Variations of local properties such as membranes thickness (distance between

phosphates of vertically adjacent PCs) or lipid tilt and ordering, are evaluated by comparing their values for distal and proximal lipids. Proximal lipid (PC or Chol) molecules are those closer than 0.8 nm to a fullerene particle. In general, distal lipids in fullerene-containing bilayers exhibit statistically equal properties to those found in fullerene-free bilayers. Small variations are found for proximal lipids. For instance, fullerenes increase the membrane thickness of DUPC membranes up to a maximum of 2.5% whereas for POPC or DPPC bilayers a tiny reduction (<1.5%) is observed. Cholesterol molecules are slightly more altered by fullerenes than PCs. The distance between Chol hydroxyl groups at opposite leaflets is increased for DUPC membranes in a large extent (up to 8%), whereas in POPC and DPPC membranes such distance is reduced up to a maximum 7%. Tilt of PC tails and Chol backbone are slightly increased for proximal lipid molecules with consistent but small increments <5%. Cholesterol-containing membranes exhibit the largest lipid tilt increments upon fullerene insertion. Alteration of lipid tail ordering is statistically negligible.

3.4 Lipid and fullerene lateral diffusion.

Dynamic properties are affected by fullerene insertion to a larger extent than structural ones. For instance, we have examined the lateral diffusion of lipids and fullerenes in the bilayer plane by measuring the diffusion coefficient

$$D_i = \lim_{t \to \infty} \left[\frac{\langle r(t)^2 \rangle_{i,t}}{4t} \right]$$

where $\langle r(t)^2 \rangle_{i,t}$ is the mean-square displacement (MSD) of the center of mass of a molecule in the xy plane averaged over all molecules of type *i* in the membrane. Because each monolayer in the membrane can drift during the simulation, the motion of the center of mass of individual leaflets is eliminated from the computation of the lipid MSD. The mean-square displacements for

a DUPC membrane system with different amounts of fullerene are presented in Fig. 7 as examples. For some simulated systems that display a clear linear regime, the lateral diffusion coefficients can be computed and they are provided in Table 2.

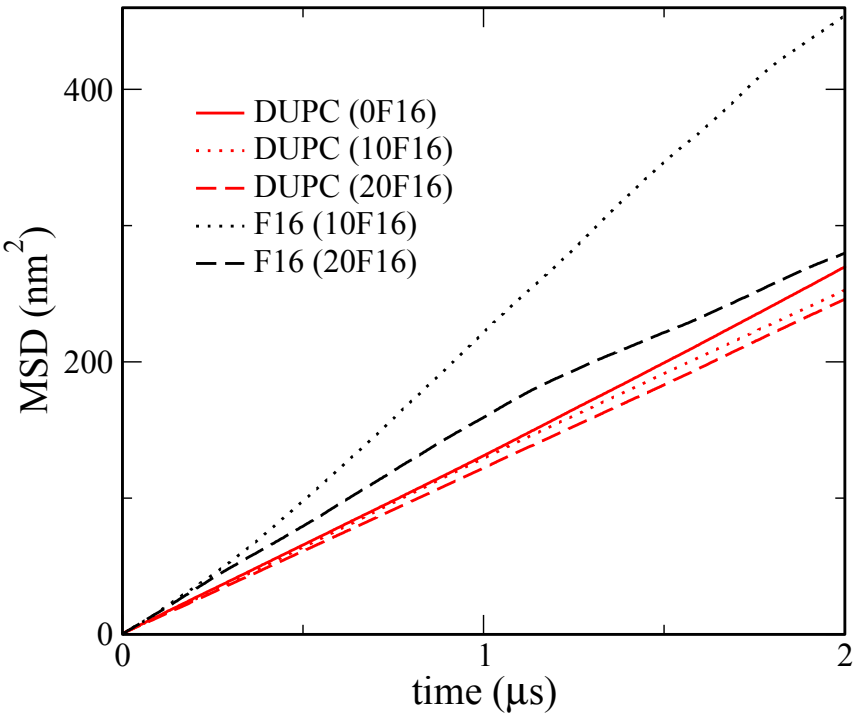

Figure 7. Mean square displacement (MSD) for DUPC (red curves) and fullerene (black curves) molecules in the simulated pure DUPC membrane (solid), and DUPC/10F16 (dotted) and DUPC/20F16 (dashed) systems. The MSD is computed once all fullerene molecules (if present) have been transferred to the hydrophobic membrane region.

Lateral diffusion rate of DUPC in a pure membrane is of the order of several 10^{-7} cm^2 s^{-1} (Table 2) that corresponds to typical phospholipid mobilities in highly disordered phases according to

experiments [41] and other coarse-grained simulations [42]. POPC and DPPC lipids forming more ordered phases display a mobility reduced by a factor of 2, in agreement with the experimental observations [43,44]. Addition of 30%mol Chol reduces by 2-3 the PC diffusivity, and up to 4 times for 50%mol Chol [43,44]. Cholesterol molecules exhibit diffusion coefficients in the range 10-26·10^{-8} cm^2 s^{-1}, displaying the smaller values when mixed with more saturated PCs. Lateral diffusivities provided here are also in agreement with mobilities obtained in other CG MD simulations [34,42].

Fullerene lateral diffusion is strongly dependent on the membrane composition (Table 2). The largest mobilities are found for DUPC bilayers and can be reduced up to 4 times when changing to DPPC or POPC, or by adding Chol. Interestingly, fullerene addition also reduces the self-diffusion constants of PCs and Chols by obstructing their lateral transport. In turn, other fullerenes are also slowed down (see Table 2).

Table 2. Lateral diffusivities for some simulated systems.[a]

	DUPC			POPC		
D_{PC}	34.5±0.4	*31.8±0.6*	**30.1±0.3**	17.0±0.5	*15.3±0.4*	**14.0±0.5**
D_{F16}	-	*47.1±2*	**38.6±1**	-	*15.9±2*	**14.8±1**
	DUPC/30%Chol			DPPC		
D_{PC}	17.7±0.5	*16.3±0.6*	**14.8±0.5**	17.6±0.4	*15.8±0.*	**14.9±0.5**

					5	
D_{F16}	-	*17.4±2*	**13.9±1**	-	*13.2±2*	**10.7±1**
D_{Chol}	26.8±0.8	*25.3±0.7*	**18.5±0.7**			

[a]Diffusion constants were computed from the linear fitting of the mean squared displacement in the 2.8–4.8 μs period and they are provided in 10^{-8} cm^2 s^{-1}.

[b]Values in italics and bold correspond to the systems with 10 and 20 fullerenes, respectively.

3.5 Alteration of cholesterol flip-flop.

Fullerene causes important effects on the transport of Chol across DUPC membranes (flip-flop). In such highly disordered bilayers, polar Chol hydroxyl beads can be significantly found close to the bilayer center (see Fig. 8), indicating a high propensity to flip-flop from one leaf to the other. Interestingly, addition of increasing amounts of fullerene systematically reduces the OH density at the central region of the bilayer (Fig. 8), suggesting that the presence of fullerene molecules in this bilayer region makes Chol rotation and subsequent flip-flop translocation more difficult. The analysis of transmembrane transport was performed by tracking the orientation of individual lipid molecules every 200 ps during a simulation period of 1 μs. No phospholipid flip–flop occurred in any of the simulated membranes, in agreement with the slow phospholipid passive translocation measured experimentally (from hours to days) [45]. Instead, recent experimental evidence suggested that chol flip–flop takes place on the submicrosecond timescale [46]. Visual inspection of the orientation of some Chol molecules reveals that they are able to eventually enter the bilayer interior adopting a horizontal position and, either return back to the same leaflet or change the leaflet. According to our simulations, Chol translocation events take place with

rates of 9.8 and 6.0 μs^{-1} for DUPC/30%Chol and DUPC/50%Chol membranes, respectively (Table 3), showing a good agreement with other molecular CG simulations [34,47]. Importantly, addition of fullerene in both cases slows down transmembrane Chol transport. As a consequence of fullerene blocking Chol rotation, flip-flop rates are decreased about a 30-40% (see Table 3), confirming our rationale.

Cholesterol translocation is much less frequent in DPPC and POPC membranes, with rates of the order of 0.1-0.5 μs^{-1}. Addition of fullerenes in these systems does not exhibit any clear tendency in favor or against Chol flip-flop and longer simulations would be required to perform this analysis.

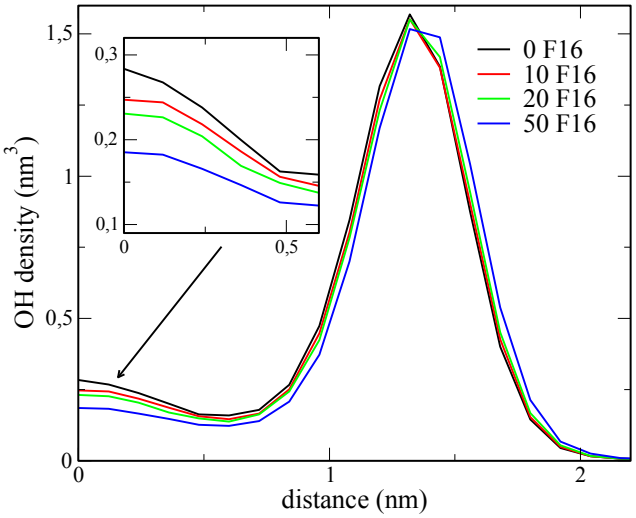

Figure 8. Cholesterol hydroxyl particle (OH) density profiles respect to the bilayer center for the DUPC/30%Chol simulated membrane systems containing different amounts of fullerene. In the inset the OH density in the central region is enlarged.

Table 3. Cholesterol flip-flop rates (μs^{-1}) for the two Chol-containing DUPC bilayers (columns) with different amounts of fullerene (rows).[a]

	DUPC/30%Chol	DUPC/50%Chol
0 F16	9.8±0.5	6.0±0.4
10 F16	9.0±0.5	5.4±0.3
20 F16	8.2±0.6	5.1±0.3
50 F16	5.6±0.5	4.2±0.4

[a]Flip-flop rates were computed by tracking the orientation of Chol molecules every 200ps during 1 μs of simulation once all fullerene molecules are transferred to the membrane interior.

3.6 Fullerene behavior in raft membranes.

Due to the relevance of raft formation in membrane biology, the behavior of fullerene in heterogeneous membranes displaying *lo*/*ld* coexistence has been analyzed. Ternary membranes with two different saturated lipids have been studied and their behavior in terms of fullerene permeabilization and translocation through the membrane shows no difference so it can be discussed -except for phase alignment between leaflets, which will be discussed later- taking as an example the DUPC/DPPC/Chol membrane (see Fig. 9). At the moment of fullerene addition,

the membrane already displays phase-segregation of a raft-like *lo* domain with molar composition 0.05/0.49/0.46 from a *ld* phase with composition 0.84/0.1/0.06. The *lo* phase occupies a 42% of the total membrane area, and the segregated phases are rather transversally aligned in the two leaflets [34]. The obtained fullerene translocation dynamics and their partitioning into the heterogeneous membrane are in agreement with the main observations reported above for homogeneous bilayers with extreme packing characteristics; namely for pure DUPC and DPPC/50%Chol systems. First, most fullerene particles penetrated the membrane rapidly (<15 ns) through the *ld* phase while those which were initially close to the *lo* domain formed aggregates and remained for longer times (≈150 ns) in the aqueous phase before being transferred to the membrane (see Fig. 9). This is consistent with what is reported in Subsections 3.1 and 3.2: fullerene molecules penetrate more easily disordered membranes (Fig. 3) than more compacted DPPC/Chol bilayers where they have to overcome a small penetration barrier (≈1.5 k_BT) at the water/lipid interface (Fig. 6). Second, once inside the bilayer, fullerene molecules and aggregates placed in a *lo* environment migrate to the *ld* phase in few tens of nanoseconds and become dissolved in the disordered membrane region (Fig. 9). The preference of fullerene for the *ld* lipid environment is clear. As an example the last snapshot of Fig. 9 shows four fullerene molecules that have become trapped inside the raft-like domain but still preserve a few DUPC molecules surrounding them. Once inside the disordered membrane region fullerene molecules become dispersed in the central bilayer segment as observed in homogeneous DUPC membranes. The preference to be placed in a disordered environment is justified by the difference in energy stabilization between DUPC and DPPC/50%Chol membranes that is of the order of 15 k_BT in favor of the disordered bilayer (Fig. 6).

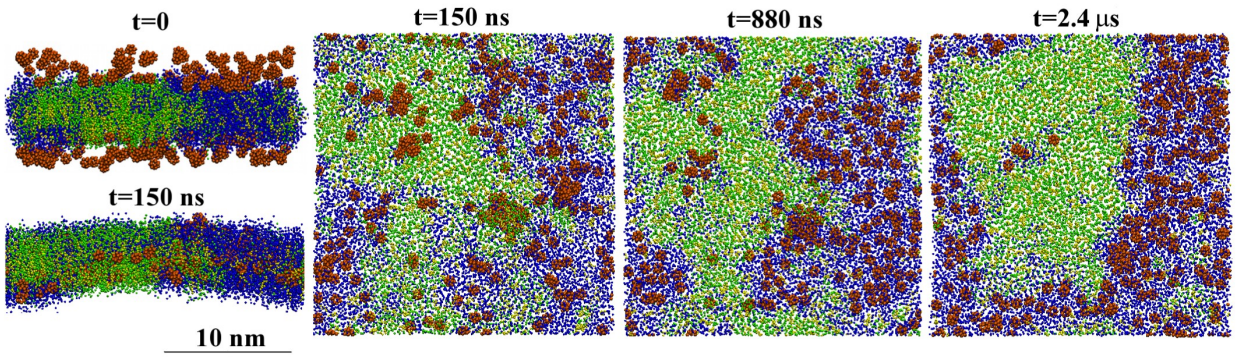

Figure 9. Temporal sequence (lateral and frontal views) for the raft-like simulated membrane displaying *lo*/*ld* coexistence. Liquid-ordered phase is rich in DPPC (green) and Chol (yellow), whereas DUPC (blue) forms the liquid-disordered phase. 200 fullerene molecules (orange) are initially placed in the aqueous phase, they all have already entered into the membrane at t=150 ns, and rapidly migrate to the disordered membrane phase. Water molecules are not shown for clarity.

The impact of fullerene on the lipid mixture phase stability is also analyzed. Notice that although the ternary mixtures are simulated at a temperature low enough to be paced at the *lo*/*ld* coexistence region of the phase diagram, the segregated patterns exhibit rather irregular and changing domains indicating the proximity with the critical conditions. Visual inspection of the sequence of frontal views in Fig. 10 shows how the addition of fullerene and its adsorption in the membranes clearly make the segregated domain more robust and regularly shaped, thus suggesting a fullerene-mediated stabilization of the *lo*/*ld* coexistence region of the mixture phase diagram. Fullerene-mediated phase stabilization was recently reported in a comparative analysis performed by MD simulations about the influence of different hydrophobic compounds acting on segregated membranes [48] which conclusion was that hydrophobic aliphatic compounds promote lipid mixing whereas hydrophobic aromatic species (including fullerene) stabilize

lateral *lo*/*ld* phase-segregation. Here this latter effect is reproduced in the two simulated raft-like membrane systems (compare Figs. 10a and 10b, and Figs. 10c and 10d), and we have quantified it by means of the lateral segregation parameter Φ. In the absence of fullerene, the ternary membranes with DPPC and DSPC lead to a fraction of lateral neighboring pairs of the same lipid phase of 79 and 83%, respectively, indicating phase separation in both cases. Addition of fullerene significantly increases the value of Φ in both raft membrane cases (see the upper panel of Fig. 10e). For the DUPC/DPPC/Chol bilayer, the translocation of 200 fullerene particles to the membrane implies an increment of a 7% of lateral contacts between lipids forming the same segregating phase, whereas for the DUPC/DSPC/Chol bilayer this increment is of a 4%.

Even more relevant than the effect on lateral segregation is the impact produced on the correlation between the layers of the membrane. In the absence of fullerene, the membrane containing DPPC presents domain alignment (registration, Fig. 10a) whereas the bilayer containing DSPC displays a clear antiregistration behavior (Fig. 10c). Quantification in terms of transversal registration percentage yields to a 64% of phase coincidence for the membrane with DPPC whereas this percentage is reduced to 41% for the bilayer with DSPC. These results can be easily explained by the competition between surface and line interdomain tensions [34, 39, 49]. A piece of membrane with the two leaflets in a *lo* phase made of DSPC and Chol molecules is significantly thicker than the *ld* phase composed by DUPC lipids. Such thickness mismatch plays against transmembrane colocalization of equal phases and promotes phase asymmetry in the DUPC/DSPC/chol system. Instead, the thickness of *lo*-*lo* transversal pairs in the DUPC/DPPC/Chol system is similar to the thickness of a DUPC *ld* membrane patch, so phase alignment is favoured in this case [34, 39]. The simulations for the two ternary segregated

systems have been extended in the presence of 100 and 200 fullerene molecules that became totally absorbed by the bilayer after a few hundred of nanoseconds. Visual inspection of the equilibrated fullerene-containing bilayer systems plotted in Fig. 10b and Fig 10d reveals the powerful influence of fullerene to promote phase registration in contrast to the same membrane in the absence of this compound. The coupling parameter Λ increases in each of the simulated membranes when fullerene is added to the system (bottom panel of Fig. 10e). The effect is quantitatively significant for the case with DPPC, and dramatic for the DUPC/DSPC/chol membrane: addition of 200 fullerene molecules increases the area registration percentage to a 66%, converting a clear antiregistration behavior into a symmetric transversal configuration. The observed synchronization effect was already reported for other chemical species like chloroform, and its molecular mechanism is based on the same entropic origin as for this compound [34, 49]. According to the PMF calculations reported in Subsection 3.2, no energy barrier is obtained for fullerene molecules in order to translocate from one leaflet to the other (Fig. 6b). As a consequence, the transversal coincidence of disordered domains where fullerene molecules are preferentially placed favors their transversal dynamics and avoids their confinement in one leaflet [34, 49].

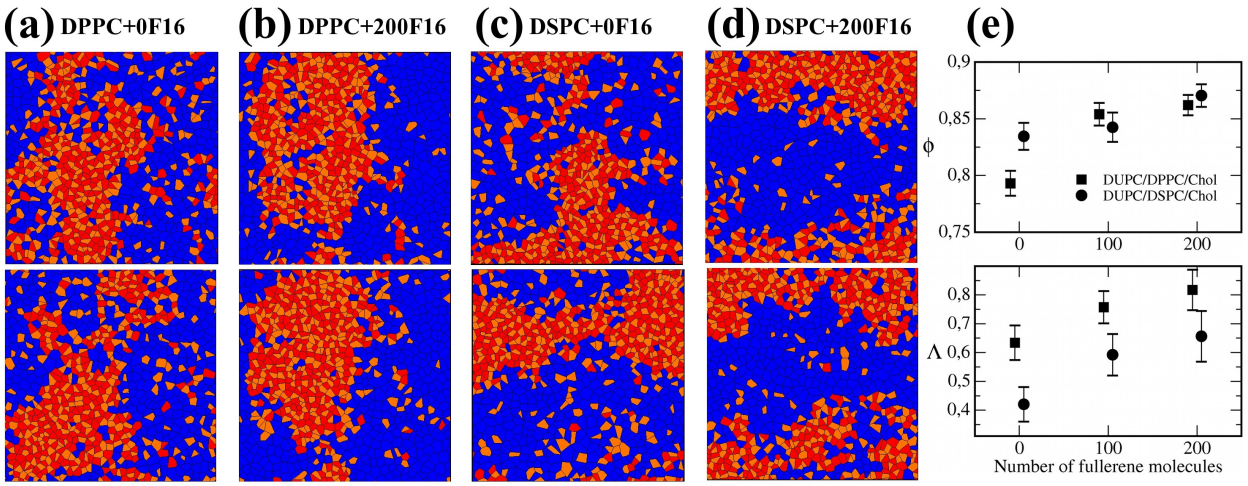

Figure 10. Final snapshots (t=4.8 μs) of each leaflet (upper and lower panels) of the simulated DUPC/x/chol membrane systems. Voronoi polygons are filled with a colour that identifies each of the lipid components: DUPC (blue), saturated lipid x (red) and Chol (orange). Saturated PC and Chol segregate in a more packed phase (*lo*) than the one formed by DUPC (*ld*). (a) x=DPPC and absence of fullerene. (b) x=DPPC and 200 fullerene molecules. The presence of fullerene stabilizes phase segregation. (c) x=DSPC and absence of fullerene. (d) x=DSPC and 200 fullerene molecules. Phase antiregistration obtained in panel (c) is reversed to domain alignment due to the effect of fullerene. (e) Segregation parameter Φ and interleaflet coupling parameter Λ for the two simulated raft systems depending on the fullerene content.

4. CONCLUSIONS

We have reported the results from CG-MD simulations of membranes with different lipid composition subjected to the effect of fullerene. The analysis of the simulations has unveiled the main molecular aspects that explain these effects and they are summarized as follows. We observe that disordered membranes formed by highly unsaturated lipids (DUPC) adsorb and dis-

solve fullerene molecules more rapidly than bilayers of monounsaturated (POPC) or saturated (DPPC) phospholipids that display higher internal ordering. Once inside the bilayer, fullerene molecules occupy the central region of a disordered membrane, whereas ordered ones host fullerene at a distance of 1.1-1.2 nm from the bilayer center. The computed energy profiles confirm the existence of an energy minimum at the location where the fullerene density profile exhibit its maximum for each membrane type. Energy profiles also reveal that DUPC membranes stabilize dispersed fullerene molecules in their interior to a larger extent than POPC and DPPC membranes. We have also reported that the presence of cholesterol, an ubiquitous lipid in biological membranes, slow down fullerene adsorption in the bilayer and reduces the ability of the bilayer to disperse fullerene in the monomeric form. Furthermore, non-favorable interactions between fullerene and cholesterol decrease the energy gain associated to the adsorption of fullerene in the membrane. So far, these results may have implications in recent experimental strategies that use liposomes for dissolving fullerene and delivering it to cells [20,21]. In these systems, fullerene molecules become placed in the liposome bilayer whose chemical affinity for fullerene can be controlled by varying its lipid composition. Thus, findings from our study can be important in the context of the development of lipid membranes as biocompatible and tunable solvent for fullerenes that may be employed in biochemical applications.

From a biological perspective, the effect of fullerene on cell membranes is a fundamental issue, and its analysis has to take into account the large diversity of lipids forming biological membranes. In particular, cholesterol-containing membranes have to be considered. Our results contribute to a better understanding of the influence of fullerene on bilayers with different lipid composition and internal ordering. Although structural membrane properties (thickness, area, lipid ordering, etc.) are not strongly altered by the presence of fullerene, molecular dynamic

characteristics are significantly modified. Lipid lateral diffusion is slowed down, and cholesterol molecules in a disordered lipid environment reduce their flip-flop frequency. Modification of Cholesterol translocation rates may affect the mechanical response to changes in membrane shape, as well as many cellular functions where Chol asymmetric distribution in the two leaflets is important.

Another important aspect is that in cell membranes lipids are distributed heterogeneously forming nanometric liquid-ordered (*lo*) domains (rafts) embedded in a liquid-disordered (*ld*) phase. With this context in mind, we have reported the effect of fullerene on membrane presenting *lo*/*ld* coexistence, and some important conclusions can be extracted. Mainly, fullerene particles may be transferred from the aqueous solution to any of the two membrane environments, but as soon as they are inside they migrate and accumulate in the disordered regions of the membrane. Our results suggest therefore that accumulation of fullerene on cell membranes may take place preferentially on those regions exhibiting the highest internal disordering. Such preference and the corresponding fullerene-mediated effects may induce changes in lipid raft organization of biological membranes and modify their properties and functionality. First, our simulations show that addition of fullerene stabilizes lateral *lo*/*ld* segregation in phase-separating membranes. Second, and more remarkably, fullerene incorporation promotes the correlation of the segregating lipid domains in the two leaflets of the bilayer. This finding contributes to the discussion about the biological impact of fullerene by introducing a new aspect: the action of fullerene could not only be related to the alteration of the lateral (in surface) lipid-protein organization but also to changes in the transversal organization of the bilayer. The correlation of lipid domains in the two leaflets of the bilayer is important to

understand many relevant biological functions taking place in the cell membrane, for example, the mechanism by which proteins on both sides of the membrane co-localize during signaling events [50], the activity of particular ion channels [51] or inserted transmembrane proteins [52] or the transversal spatial coincidence of specific lipid phases required in immunological responses [53]. How the presence of fullerene may alter the phase cross-talk between the two leaflets of the membranes is therefore of key importance to understand its impact on the biological function.

Conflicts of interests

The authors declare no conflict of interest.

Acknowledgements

Authors acknowledge financial support from Spanish Ministry of Economy and Competitiveness (MINECO) through project FIS 2013-41144P and through the "Severo Ochoa" Programme for Centres of Excellence in R&D (SEV-2015-0522). Authors also acknowledge financial support from Fundació Privada Cellex, and CERCA Programme / Generalitat de Catalunya.

REFERENCES

[1] J. Zhang, M. Terrones, C.R. Park, R. Mukherjee, M. Monthioux, N. Koratkar, Y.S. Kim, R. Hurt, E. Frackowiak, T. Enoki, Y. Chen, Y. Chen, A. Bianco, Carbon science in 2016: status, challenges and perspectives, Carbon 98 (2016) 708-732.

[2] F. Piccinno, F. Gottschalk, S. Seeger, B. Nowack, Industrial production quantities and uses of ten engineered nanomaterials in Europe and the world, J. Nanopart. Res. 14 (2012) 1109.

[3] R.H. Hurt, M. Monthioux, A. Kane, Toxicology of carbon nanomaterials: status, trends, and perspectives on this special issue, Carbon 44 (2006) 1028-1033.

[4] H.F. Krug, P. Wick, Nanotoxicology: an interdisciplinary challenge, Angew. Chem. Int. Ed. 50 (2011) 1260–1278.

[5] G. Oberdörster, J. Ferin, E. Lehnert, Correlation between particle size, in vivo particle persistence, and lung injury, Environ. Health Perspect. 102 (1994) 173-179.

[6] G. Oberdörster, Z. Sharp, V. Atudorei, A. Elder, R. Gelein, W. Kreyling, C. Cox, Translocation of inhaled ultrafine particles to the brain, Inhal. Toxicol. 16 (2004) 437-445.

[7] G. Oberdörster, E. Oberdörster, J. Oberdörster, Nanotoxicology: an emerging discipline evolving from studies of ultrafine particles, Environ. Health Perspect. 113 (2005) 823-839.

[8] H.B. Wang, R. DeSousa, J. Gasa, K. Tasaki, G. Stucky, B. Jousselme, F. Wudl, Fabrication of new fullerene composite membranes and their application in proton exchange membrane fuel cells, J. Membr. Sci. 289 (2007) 277-283.

[9] T. Wharton, L.J. Wilson, Toward fullerene-based X-ray contrast agents: design and synthesis of non-ionic, highly-iodinated derivatives of C60, Tetrahedron Letters 43 (2002) 561-564.

[10] C. Wang, L.A. Tai, D.D. Lee, P.P. Kanakamma, C.K-F. Shen, T-Y. Luh, C.H. Cheng, K.C. Hwan, C_{60} and water-soluble fullerene derivatives as antioxidants against radical-initiated lipid peroxidation, J. Med. Chem. 42 (1999) 4614-4620.

[11] J.J. Ryan, H.R. Bateman, A. Stover, G. Gomez, S.K. Norton, W. Zhao, L.B. Schwartz, R. Lenk, C.L. Kepley, Fullerene nanomaterials inhibit the allergic response, J. Immunol. 179 (2007) 665-672.

[12] I. Kopova, L. Bacakova, V. Lavrentiev, J. Vacik, Growth and Potential Damage of Human Bone-Derived Cells on Fresh and Aged Fullerene C_{60} Films, Int. J. Mol. Sci. 14 (2013) 9182-9204.

[13] H. Murayama, S. Tomonoh, J.M. Alford, M.E. Karpuk, Fullerene production in tons and more: from science to industry, Fuller. Nanotub. Carbon Nanostruct. 12 (2004) 1-9.

[14] BCC Research. http://www.bccresearch.com/market-research/nanotechnology/nanocomposites-nanoparticles-nantubes-market-report-nan021g.html (March 18, 2017).

[15] V.L Calvin, The potential environmental impact of engineered nanomaterials, Nature Biotechnol. 21 (2003) 1166-1170.

[16] C.M. Sayes, J.D. Fortner, W. Guo, D. Lyon, A.M. Boyd, K.D. Ausman, Y.J. Tao, B. Sitharaman, L.J. Wilson, J.B. Hughes, J.L. West, V.L. Colvin, The differential cytotoxicity of water-soluble fullerenes, Nano Lett. 4 (2004) 1881-1887.

[17] G. Jia, H. Wang, L. Yan, X. Wang, R. Pei, T. Yan, Y. Zhao, X. Guo, Cytotoxicity of carbon nanomaterials: single-wall nanotube, multi-wall nanotube, and fullerene, Environ. Sci. Technol. 39 (2005) 1378-1383.

[18] W-C. Hou, B.Y. Moghadam, P. Westerhoff, J.D. Posner, Distribution of fullerene nanomaterials between water and model biological membranes, Langmuir 27 (2011) 11899-11905.

[19] Y. Ha, L.E. Katz, H.M. Liljestrand, Distribution of fullerene nanoparticles between water and solid supported lipid membranes: thermodynamics and effects of membrane composition on distribution, Environ. Sci. Technol. 49 (2015) 14546-14553.

[20] Y. Chen, G.D. Bothun, Lipid-assisted formation and dispersion of aqueous and bilayer-embedded nano-C_{60}, Langmuir 25 (2009) 4875-4879.

[21] A. Ikeda, Y. Doi, M. Hashizume, J. Kikuchi, T. Konishi, An extremely effective DNA photocleavage utilizing functionalized liposomes with a fullerene-enriched lipid bilayer, J. Am. Chem. Soc. 129 (2007) 4140-4141.

[22] A. Ikeda, K. Kiguchi, T. Shigematsu, K. Nobusawa, J. Kikuchi, M. Akiyama, Location of [60]fullerene incorporation in lipid membranes, Chem. Commun. 47 (2011) 12095-12097.

[23] R. Qiao, A.P. Roberts, A.S. Mount, S.J. Klaine, Q.C. Ke, Translocation of C_{60} and its derivatives across a lipid bilayer, Nano Lett. 7 (2007) 614-619.

[24] L. Li, H. Davande, D. Bedrov, G.D. Smith, A molecular dynamics simulation study of C_{60} fullerenes inside a dimyristoylphosphatidylcholine lipid bilayer, J. Phys. Chem. 111 (2007) 4067-4072.

[25] J. Wong-Ekkabut, S. Baoukina, W. Triampo, I-M. Tang, D.P. Tieleman, L. Monticelli, Computer simulation study of fullerene translocation through lipid membranes, Nat. Nanotech. 3 (2008) 363-368.

[26] L. Monticelli, On atomistic and coarse-grained models for C_{60} fullerene, J. Chem. Theory Comput. 8 (2012) 1370-1378.

[27] J. Barnoud, G. Rossi, L. Monticelli, Lipid membranes as solvents for carbon nanoparticles, Phys. Rev. Lett. 112 (2014) 068102.

[28] M. Houslay, K.K. Stanley, *Dynamics of Biological Membranes*; Wiley: New York, 1982.

[29] K. Simons, E. Ikonen, Functional rafts in cell membranes, Nature 387 (1997) 569-572.

[30] S. Munro, Lipid rafts: elusive or illusive?, Cell 115 (2003) 377-388.

[31] K. Simons, D. Toomre, Lipid rafts and signal transduction, Mol. Cell. Biol. 1 (2000) 31-41.

[32] S.J. Marrink, H.J. Risselada, S. Yefimov, D.P. Tieleman, A.H. de Vries, The MARTINI force field: coarse grained model for biomolecular simulations, J. Phys. Chem. B 111 (2007) 7812-7824.

[33] S.J. Marrink, D.P. Tieleman, Perspective on the Martini model, Chem. Soc. Rev. 42 (2013) 6801-6822.

[34] R. Reigada, F. Sagués, Chloroform alters interleaflet coupling in lipid bilayers: an entropic mechanism, J. R. Soc. Interface 12 (2015) 20150197.

[35] I. Mannelli, F. Sagués, V. Pruneri, R. Reigada, Lipid vesicle interaction with hydrophobic surfaces: a coarse grained molecular dynamics study, Langmuir 32 (2016) 12632-12640.

[36] E. Lindahl, B. Hess, D. van der Spoel, GROMACS 3.0: a package for molecular simulation and trajectory analysis, J. Mol. Model. 7 (2001) 306–317.

[37] G.M. Torrie, J.P. Valleau, Nonphysical sampling distributions in Monte Carlo free-energy estimation: Umbrella sampling, J. Comput. Phys. 23 (1977) 187-199.

[38] J.S. Hub, B.L. de Groot, D. van der Spoel, g_wham – A free weighted histogram analysis implementation including robust error and autocorrelation estimates, J. Chem. Theory Comput. 6 (2010) 3713-3720.

[39] J.D. Perlmutter, J.N. Sachs, Interleaflet interaction and asymmetry in phase separated lipid bilayers: molecular dynamics simulations, J. Am. Chem. Soc. 133 (2011) 6563-6577.

[40] S.J. Marrink, H.J.C. Berendsen, Permeation process of small molecules across lipid membranes studied by molecular dynamics simulations, J. Phys. Chem. 100 (1996) 16729-16738.

[41] A. Filippov, G. Oradd, G. Lindblom, The effect of cholesterol on the lateral diffusion of phospholipids in oriented bilayers, Biophys. J. 84 (2003) 3079-3086.

[42] H.J. Risselada, S.J. Marrink, The molecular face of lipid rafts in model membranes, Proc. Natl. Acad. Sci. USA 105 (2008) 17367-17372.

[43] G. Lindblom, G. Orädd, Lipid lateral diffusion and membrane heterogeneity, Biochim. Biophys. Acta 1788 (2009) 234-244.

[44] N. Kahya, D. Scherfeld, K. Bacia, B. Poolman, P. Schwille, Probing lipid mobility of raft-exhibiting model membranes by fluorescence correlation spectroscopy, J. Biol. Chem. 278 (2003) 28109-28115.

[45] W.C. Wimley, T.E. Thompson, Exchange and flip-flop of dimyristoyl phosphatidylcholine in liquid crystalline, gel and two-component, two-phase large unilamellar vesicles, Biochemistry 29 (1990) 1296–1303.

[46] T.L. Steck, J. Ye, Y. Lange, Probing red cell membrane cholesterol movement with cyclodextrin, Biophys. J. 83 (2002) 2118–2125.

[47] W.F.D. Bennett, J.L. MacCallum, M.J. Hinner, S.J. Marrink, D.P. Tieleman, Molecular view of cholesterol flip–flop and chemical potential in different membrane environments, J. Am. Chem. Soc. 131 (2009) 12714-12720.

[48] J. Barnoud, G. Rossi, S.J. Marrink, L. Monticelli, Hydrophobic compounds reshape membrane domains, PLoS Comp. Biol. 10 (2014) e1003873.

[49] R. Reigada, Alteration of interleaflet coupling due to compounds displaying rapid translocation in lipid membranes, Sci. Rep. 6 (2016) 32934.

[50] K.G.N. Suzuki, T.K. Fujiwara, M. Edidin, A. Kusumi, Dynamic recruitment of phospholipase Cγ at transiently immobilized GPI-anchored receptor clusters induces IP3–Ca^{2+} signaling: single-molecule tracking study, J. Cell Biol. 177 (2007) 731-742.

[51] S.L. Keller, S.M. Gruner, K. Gawrisch, Small concentrations of alamethicin induce a cubic phase in bulk phosphatidylethanolamine mixtures, Biochim. et Biophys. Acta 1278 (1996) 241-246.

[52] W.R. Burack, R.L. Biltonen, Lipid bilayer heterogeneities and modulation of phospholipase A2 activity, Chem. Phys. Lipids 73 (1994) 209-222.

[53] S. Chiantia, E. London, Acyl chain length and saturation modulate interleaflet coupling in asymmetric bilayers: effects on dynamics and structural order, Biophys. J. 103 (2012) 2311-2319.

Graphical Abstract